

Figure S1. MR representation of the inserts embedded in the phantom, with corresponding textures and VOIs placement for different planes. (A) Axial acquisition plane; (B) Coronal reconstruction plane; (C) Sagittal reconstruction planes.



Figure S2. Ability of features to discriminate textures 1 and 2 on scanner A. For each feature, the percentage of times the feature can discriminate the two textures is reported, considering only the cases (among original and filtered images) the feature is repeatable. The maximum number of such occurrences for each feature is reported in between brackets, after the feature name.



Figure S3. Ability of features to discriminate textures 1 and 3 on scanner A. For each feature, the percentage of times the feature can discriminate the two textures is reported, considering only the cases (among original and filtered images) the feature is repeatable. The maximum number of such occurrences for each feature is reported in brackets, after the feature name.



Figure S4. Ability of features to discriminate textures 3 and 2 on scanner A. For each feature, the percentage of times the feature can discriminate the two textures is reported, considering only the cases (among original and filtered images) the feature is repeatable. The maximum number of such occurrences for each feature is reported in brackets, after the feature name.



Figure S5. Ability of features to discriminate textures 1 and 2 on scanner B. For each feature, the percentage of times the feature can discriminate the two textures is reported, considering only the cases (among original and filtered images) the feature is repeatable. The maximum number of such occurrences for each feature is reported in between brackets, after the feature name.

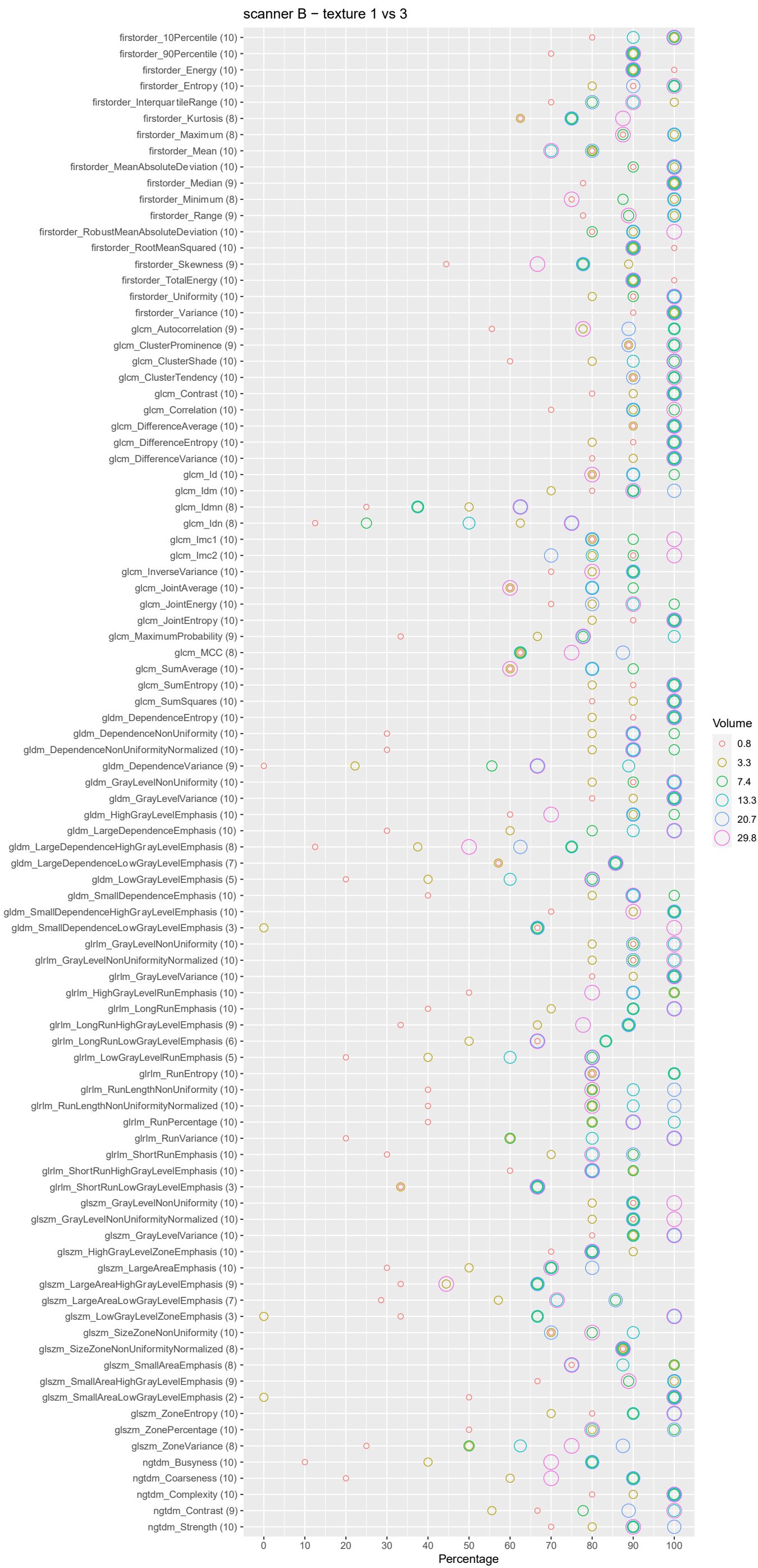


Figure S6. Ability of features to discriminate textures 1 and 3 on scanner B. For each feature, the percentage of times the feature can discriminate the two textures is reported, considering only the cases (among original and filtered images) the feature is repeatable. The maximum number of such occurrences for each feature is reported in brackets, after the feature name.



Figure S7. Ability of features to discriminate textures 3 and 2 on scanner B. For each feature, the percentage of times the feature can discriminate the two textures is reported, considering only the cases (among original and filtered images) the feature is repeatable. The maximum number of such occurrences for each feature is reported in brackets, after the feature name.

scanner C – texture 1 vs 2



Figure S8. Ability of features to discriminate textures 1 and 2 on scanner C. For each feature, the percentage of times the feature can discriminate the two textures is reported, considering only the cases (among original and filtered images) the feature is repeatable. The maximum number of such occurrences for each feature is reported in brackets, after the feature name.

scanner C – texture 1 vs 3

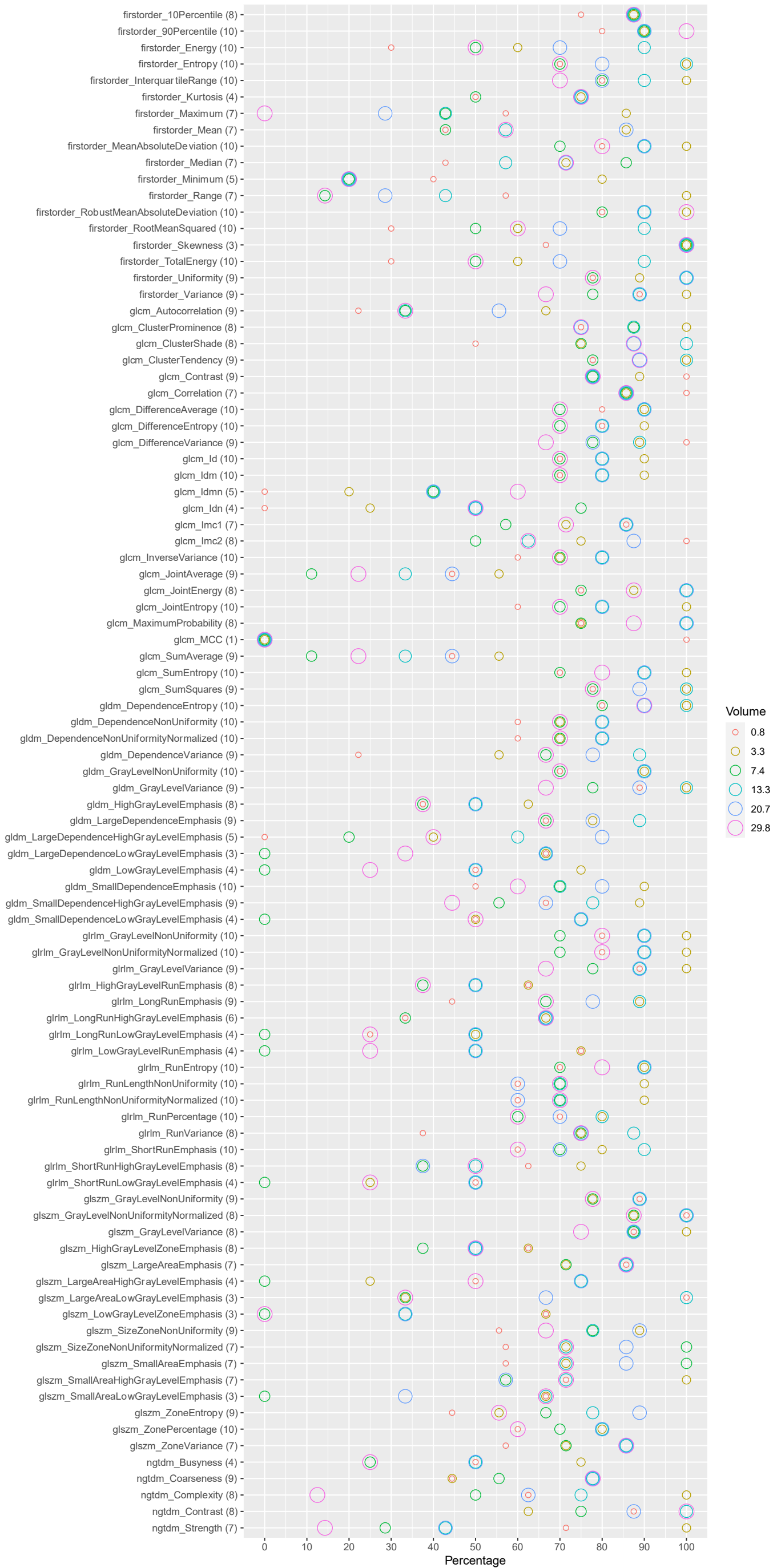


Figure S9. Ability of features to discriminate textures 1 and 3 on scanner C. For each feature, the percentage of times the feature can discriminate the two textures is reported, considering only the cases (among original and filtered images) the feature is repeatable. The maximum number of such occurrences for each feature is reported in brackets, after the feature name.

scanner C – texture 3 vs 2

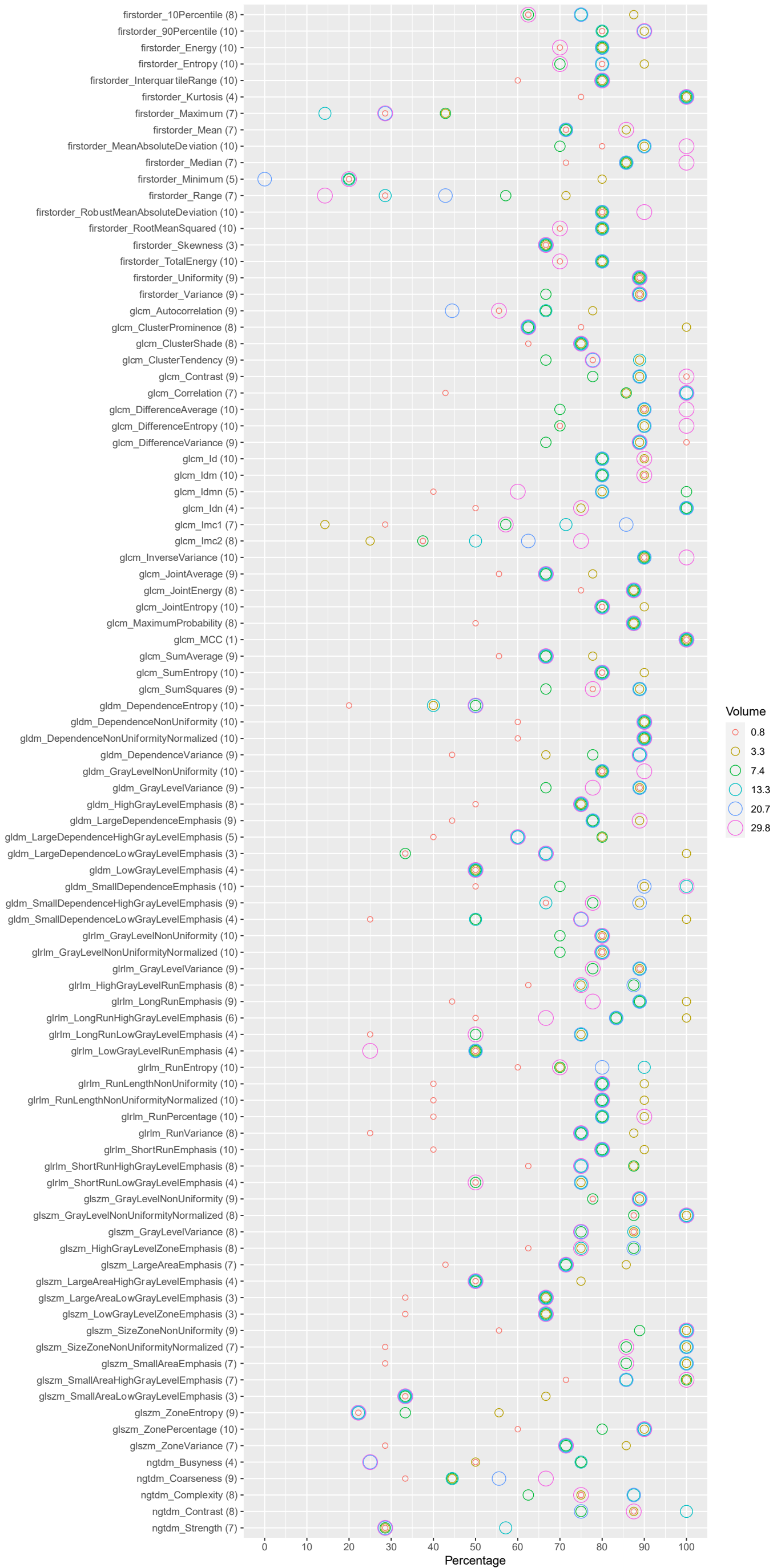


Figure S10. Ability of features to discriminate textures 3 and 2 on scanner C. For each feature, the percentage of times the feature can discriminate the two textures is reported, considering only the cases (among original and filtered images) the feature is repeatable. The maximum number of such occurrences for each feature is reported in brackets, after the feature name.

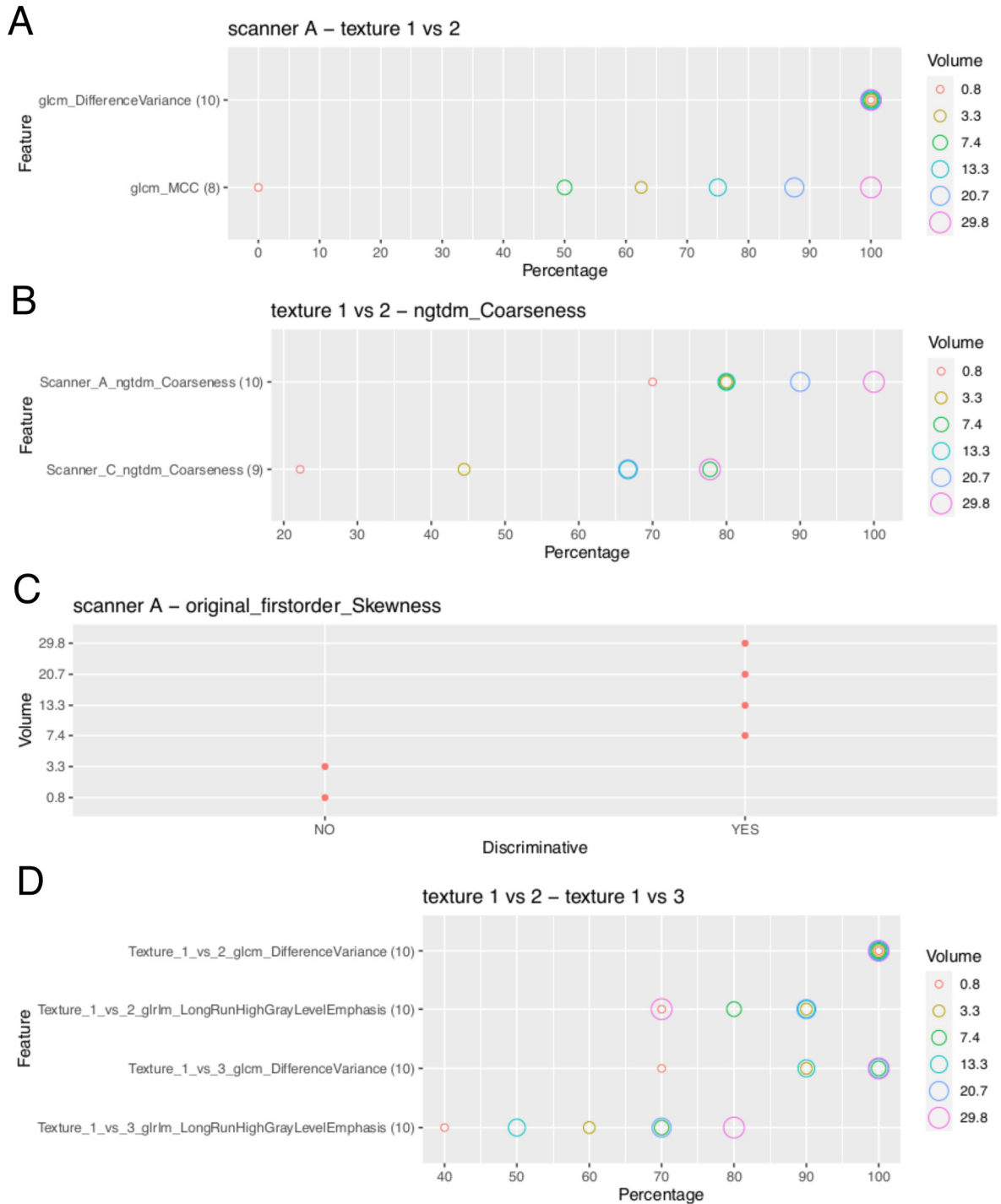


Figure S11. Examples of texture discrimination dependencies. (A) the texture discrimination for two different features (GLCM Difference Variance and GLCM MCC) at different VOI sizes; (B) dependency of texture discrimination on magnetic field strength for NGTDM Coarseness feature in scanners A and C across VOI sizes; (C) dependency of VOI size on the discriminability of textures 1 and 2 for the Original First-Order Skewness feature when calculated on original and filtered images ac-quired with scanner A; (D) discriminability difference of two features (GLCM Difference Variance and GLRLM Long Run High Gray Level Emphasis) between two different pairs of textures (1 vs 2 and 1 vs 3) as a function of the VOI size.

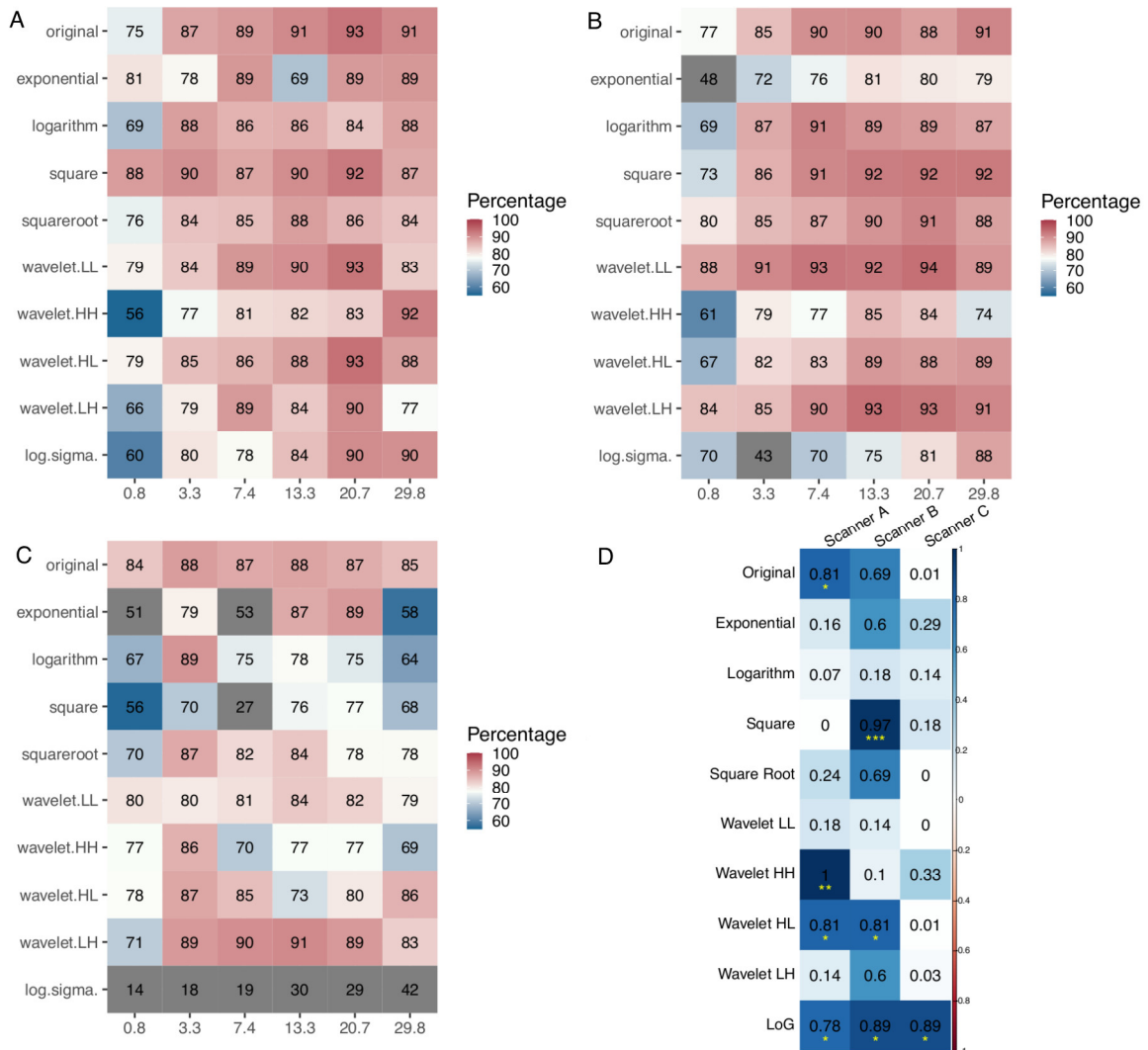


Figure S12. (A, B and C) Overall percentage of features discriminative at different volumes for each filter in scanners A - (A), B - (B), and C - (C). (D) Coefficient of determination, R-squared, of the percentage of discriminative features explained by the volume for each scanner. In (D), p-value < 0.001 is shown in yellow as ***, p-value < 0.01 is shown in yellow as **, p-value < 0.05 is shown in yellow as *.

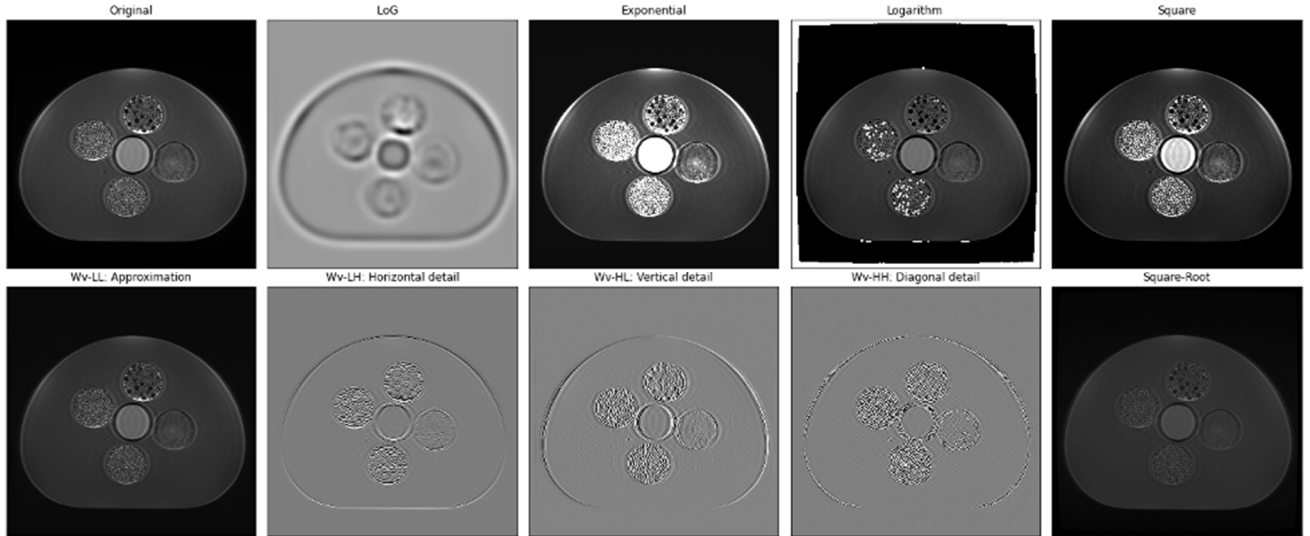


Figure S13. Representation of original and filtered images from which radiomic features were extracted. Window Width and Window Level of Exponential, Logarithm, Square, Wavelet-LL (Wv-LL) and Square Root examples were adjusted so that the aqueous solution of MnCl₂ would have similar apparent intensities to demonstrate the differences in the texture inserts. For Laplacian of Gaussian (LoG), Wavelet-LH (Wv-LH), Wavelet-LH (Wv-HL), and Wavelet-HH (Wv-HH) were adjusted to improve details enhanced by each of these filters.

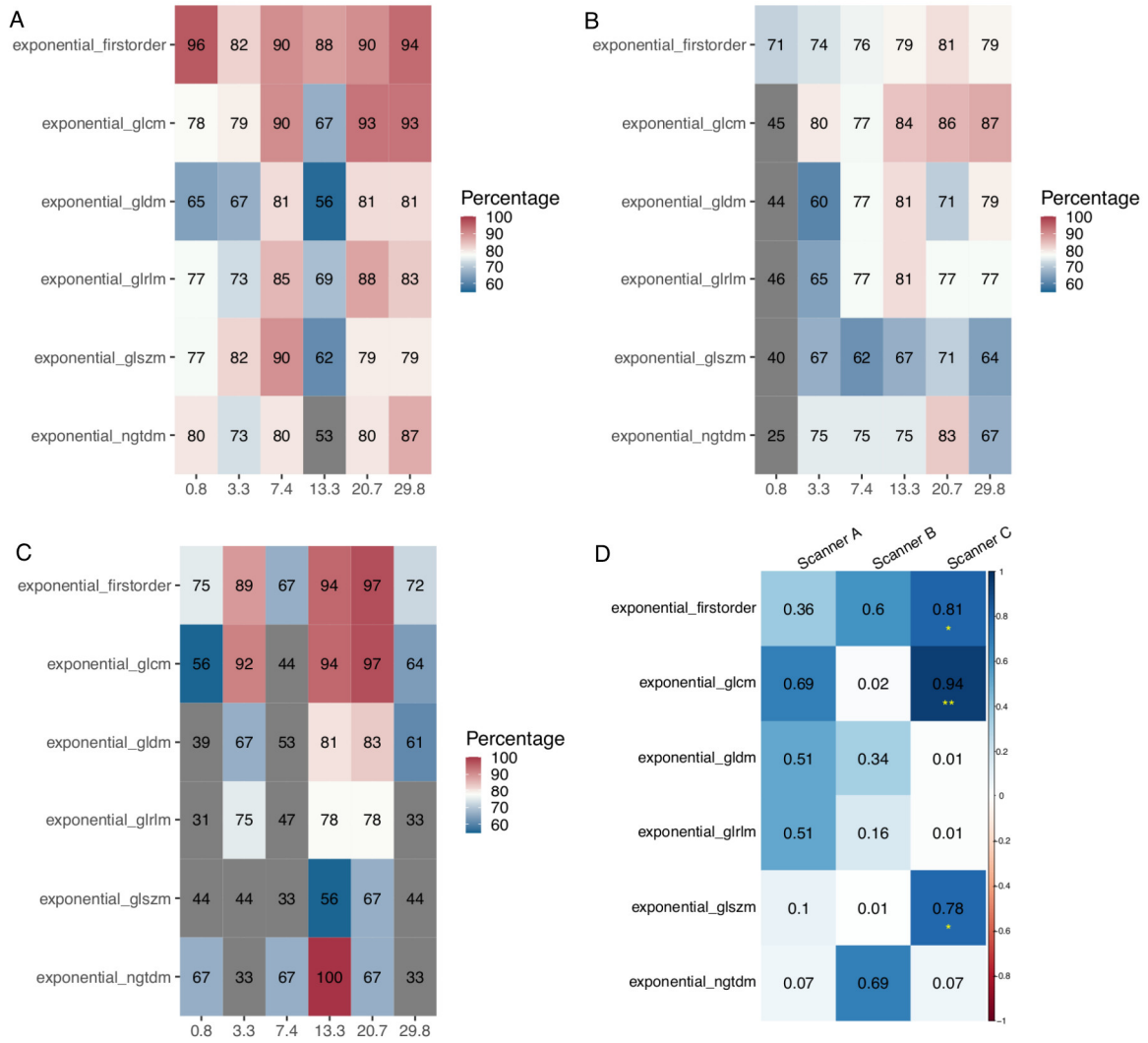


Figure S14. (A, B and C) Overall percentage of features discriminative at different volumes for each feature class extracted from the exponential filtered images in scanners A - (A), B - (B), and C - (C). (D) Coefficient of determination, R-squared, of the percentage of discriminative features explained by the volume for each scanner.

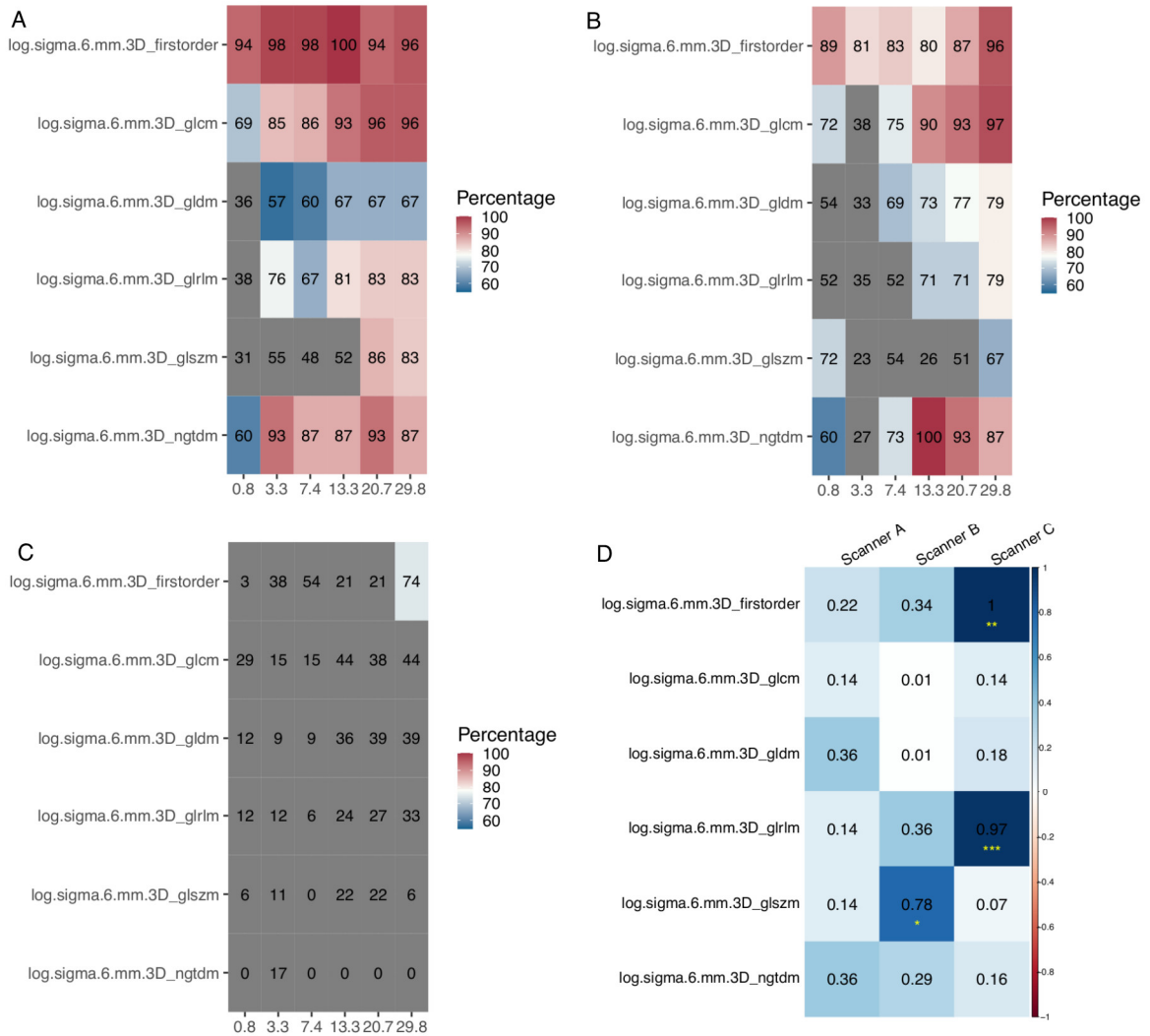


Figure S15. (A, B and C) Overall percentage of features discriminative at different volumes for each feature class extracted from the Laplacian of Gaussian ($\sigma=6\text{mm}$) filtered images in scanners A - (A), B - (B), and C - (C). **(D)** Coefficient of determination, R-squared, of the percentage of discriminative features explained by the volume for each scanner.

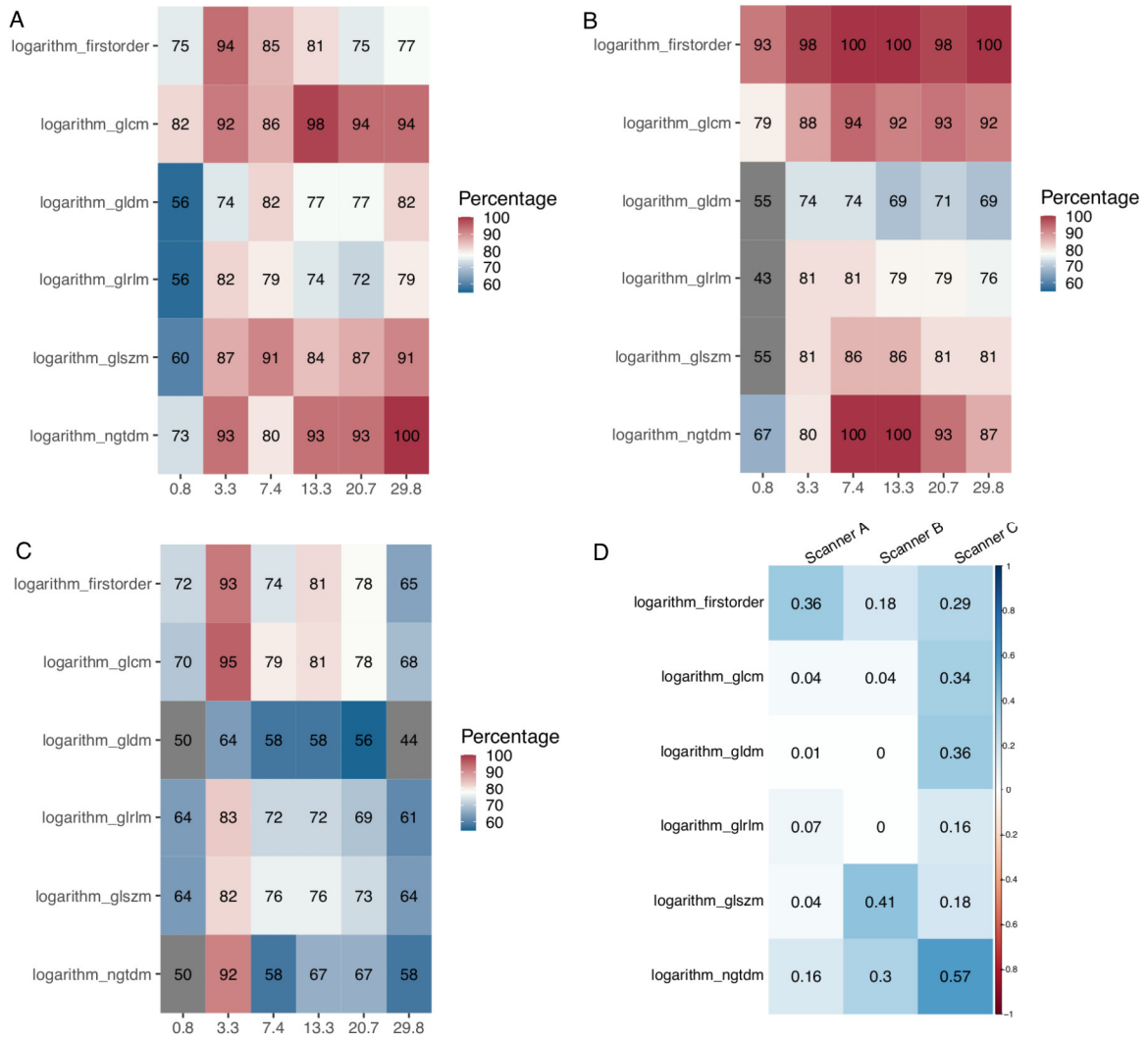


Figure S16. (A, B and C) Overall percentage of features discriminative at different volumes for each feature class extracted from the Logarithm filtered images in scanners A - (A), B - (B), and C - (C). (D) Coefficient of determination, R-squared, of the percentage of discriminative features explained by the volume for each scanner.

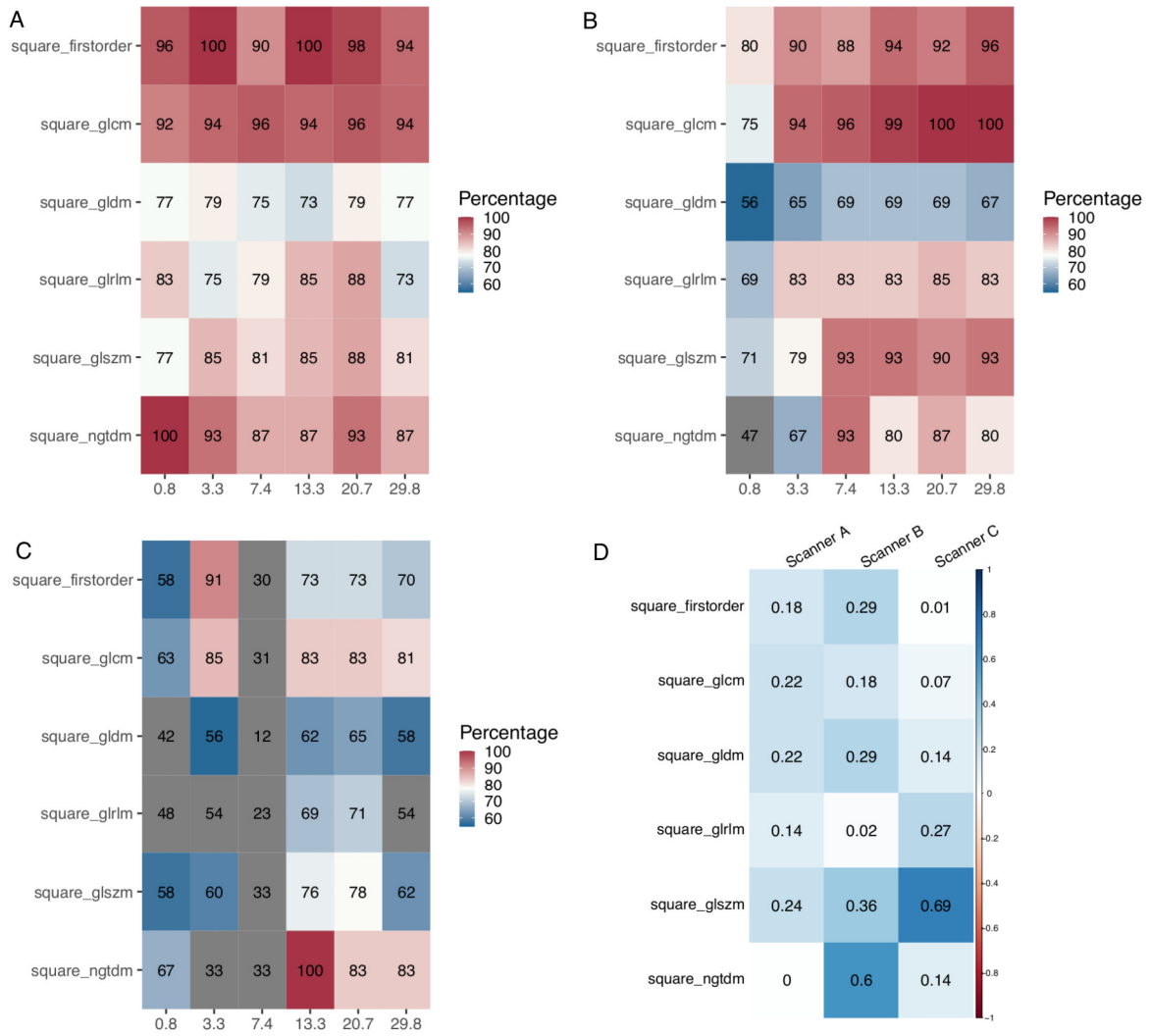


Figure S17. (A, B and C) Overall percentage of features discriminative at different volumes for each feature class extracted from the Square filtered images in scanners A - (A), B - (B), and C - (C). (D) Coefficient of determination, R-squared, of the percentage of discriminative features explained by the volume for each scanner.

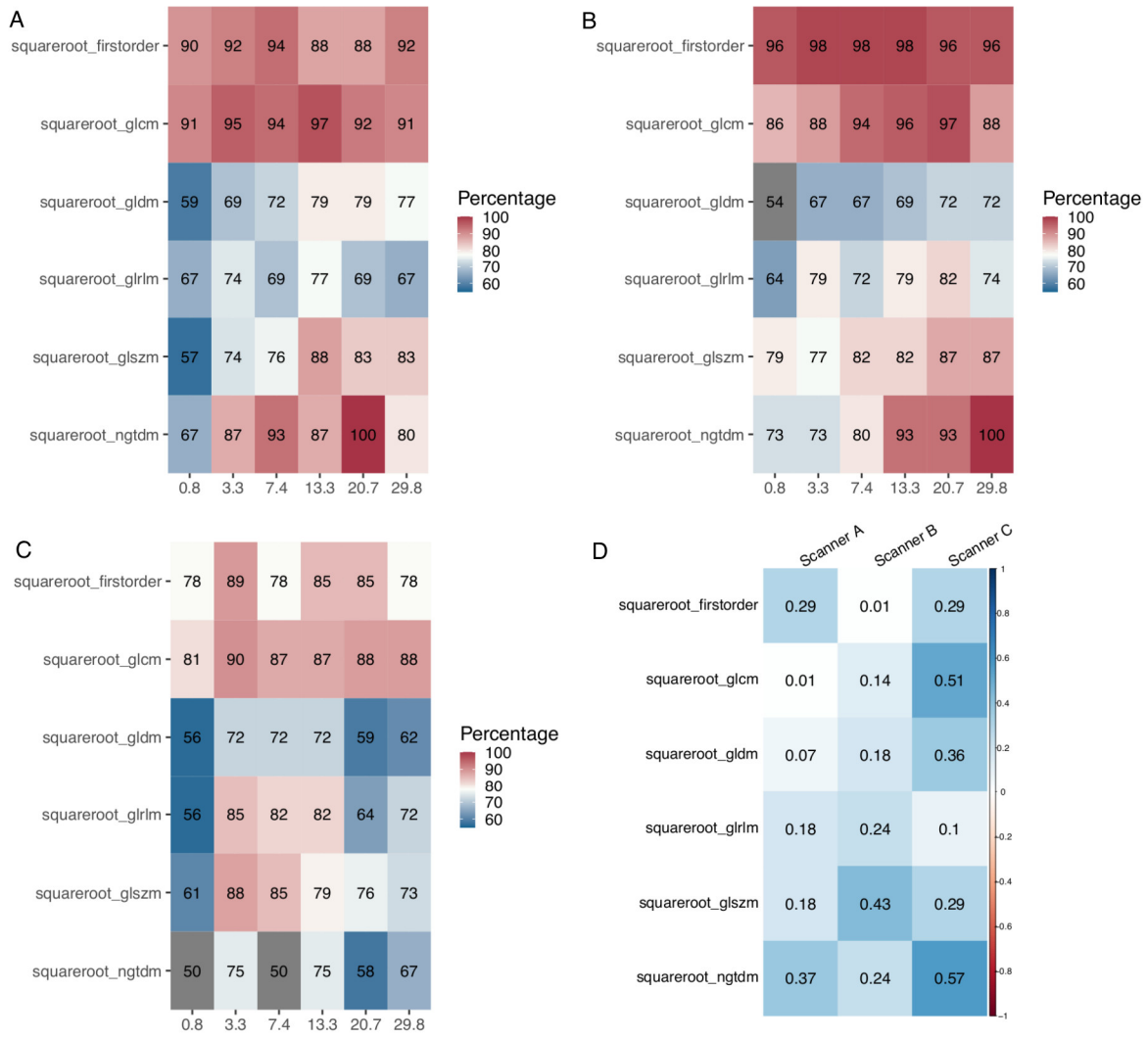


Figure S18. (A, B and C) Overall percentage of features discriminative at different volumes for each feature class extracted from the Square Root filtered images in scanners A - (A), B - (B), and C - (C). (D) Coefficient of determination, R-squared, of the percentage of discriminative features explained by the volume for each scanner.

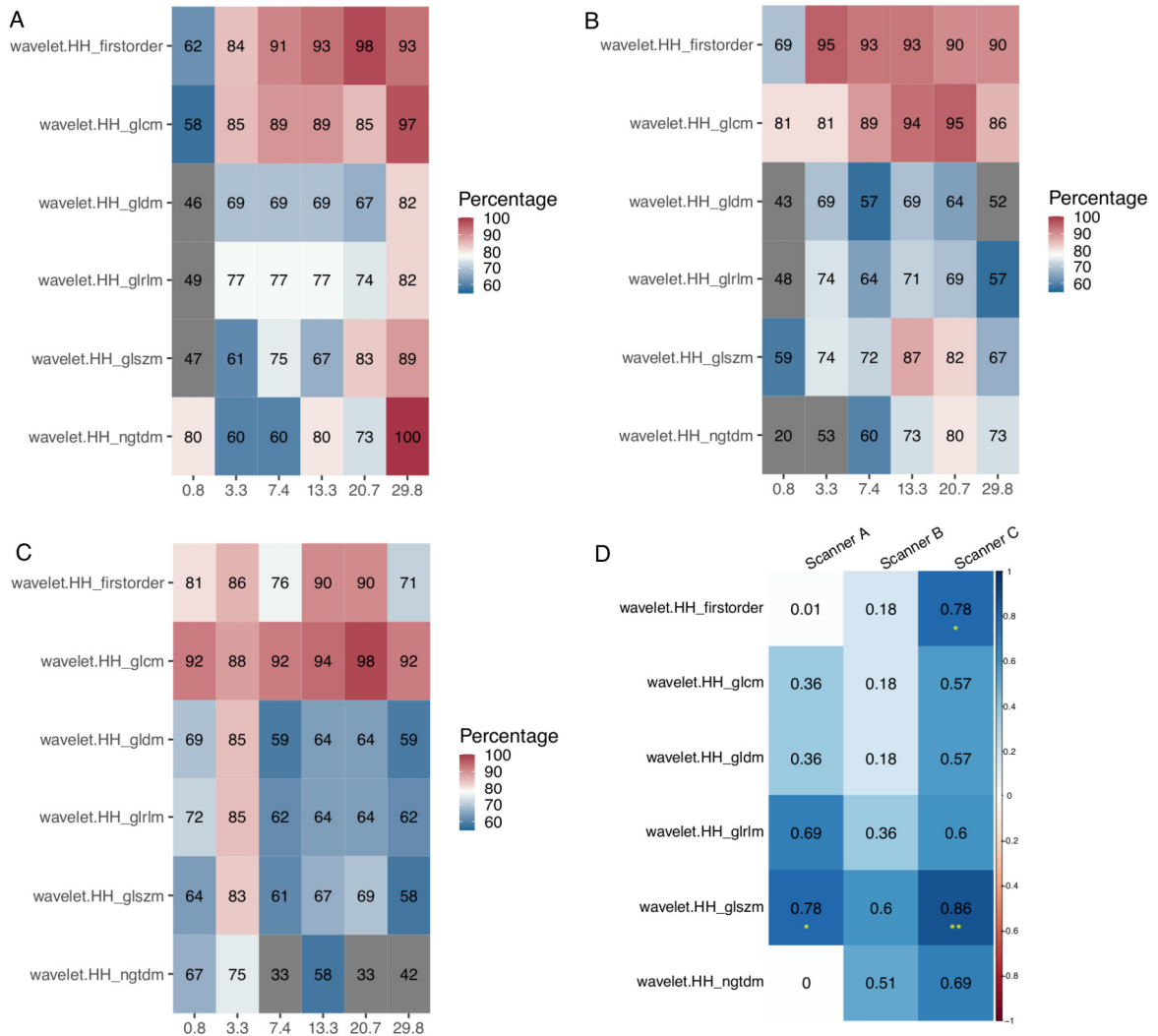


Figure S19. (A, B and C) Overall percentage of features discriminative at different volumes for each feature class extracted from the Wavelet HH decomposition filtered images in scanners A - (A), B - (B), and C - (C). **(D)** Coefficient of determination, R-squared, of the percentage of discriminative features explained by the volume for each scanner.

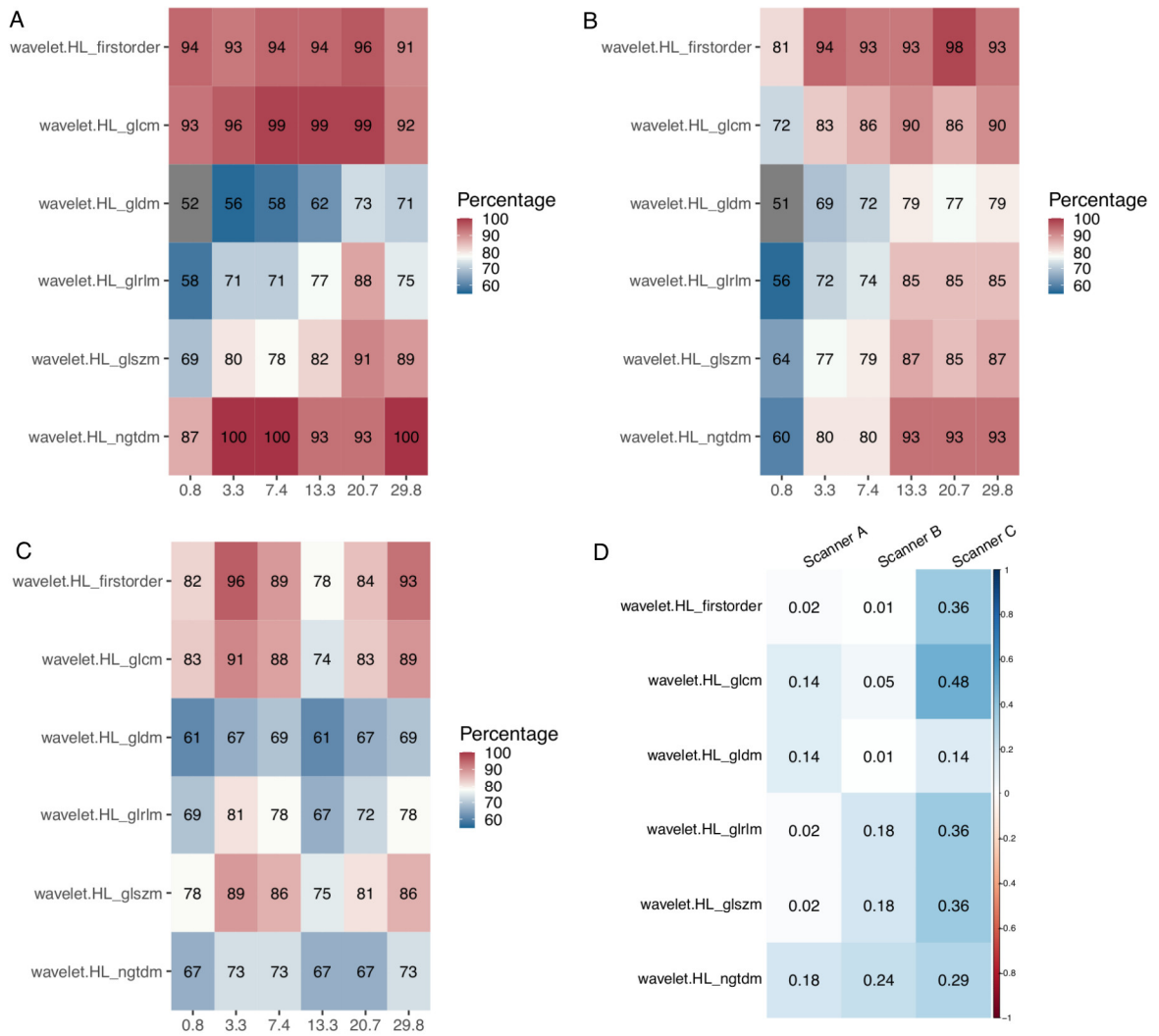


Figure S20. (A, B and C) Overall percentage of features discriminative at different volumes for each feature class extracted from the Wavelet HL decomposition filtered images in scanners A - (A), B - (B), and C - (C). **(D)** Coefficient of determination, R-squared, of the percentage of discriminative features explained by the volume for each scanner.

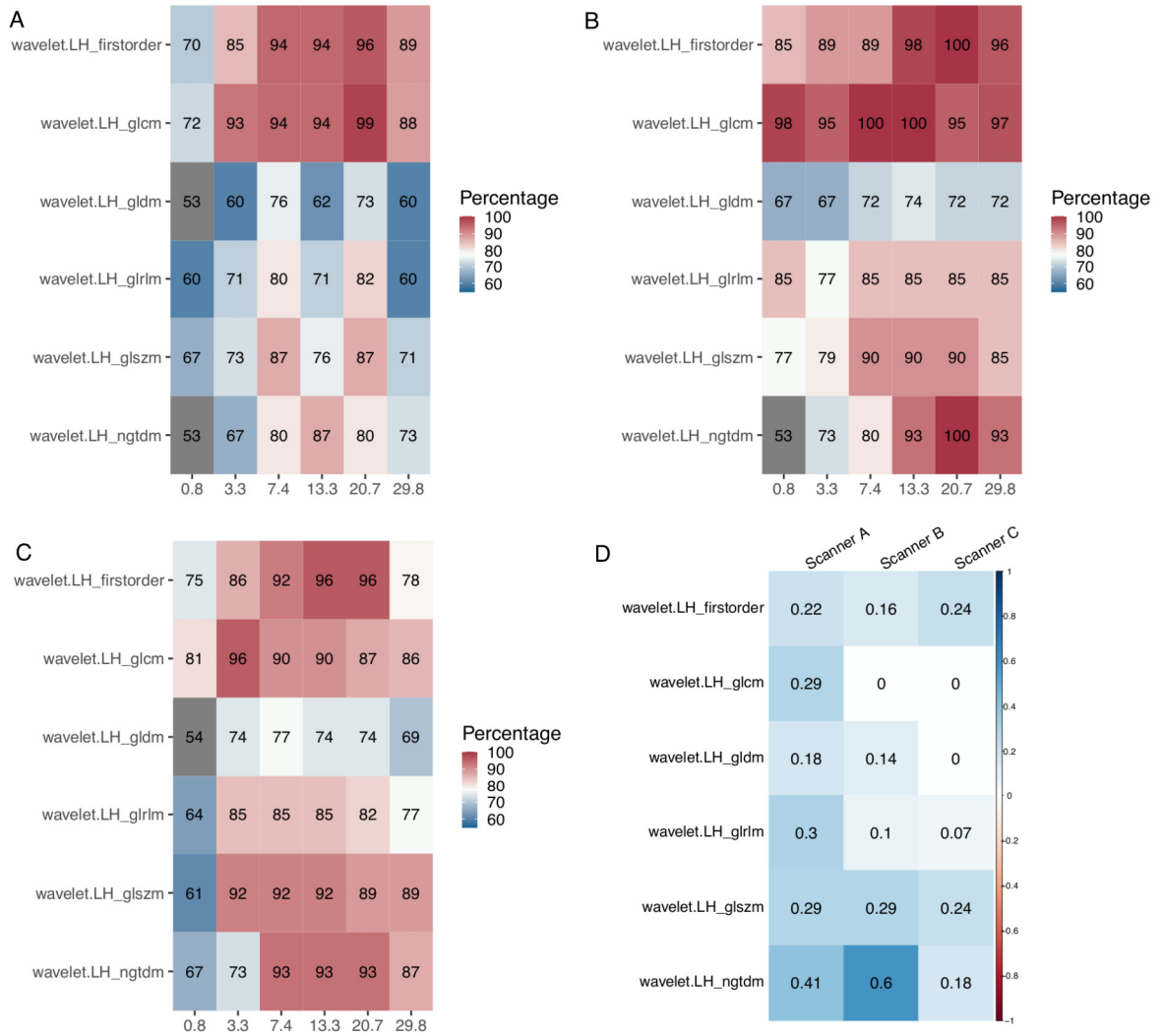


Figure S21. (A, B and C) Overall percentage of features discriminative at different volumes for each feature class extracted from the Wavelet LH decomposition filtered images in scanners A - (A), B - (B), and C - (C). **(D)** Coefficient of determination, R-squared, of the percentage of discriminative features explained by the volume for each scanner.

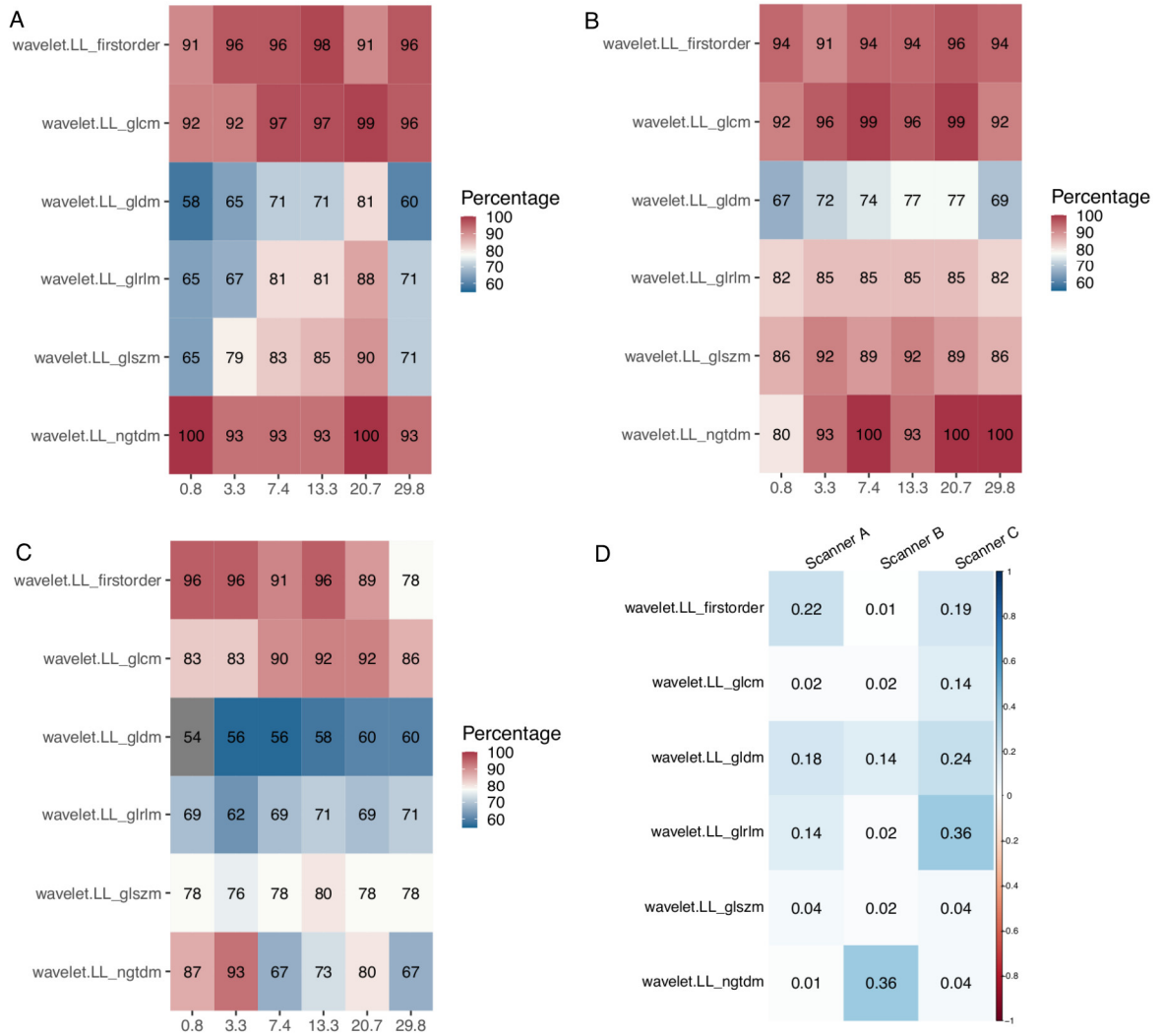


Figure S22. (A, B and C) Overall percentage of features discriminative at different volumes for each feature class extracted from the Wavelet LL decomposition filtered images in scanners A - (A), B - (B), and C - (C). (D) Coefficient of determination, R-squared, of the percentage of discriminative features explained by the volume for each scanner.